THE JOURNAL OF BIOLOGICAL CHEMISTRY VOL. 287, NO. 32, pp. 26749–26763, August 3, 2012
Published in the U.S.A.

Unveiling the Novel Dual Specificity Protein Kinases in *Bacillus anthracis*

IDENTIFICATION OF THE FIRST PROKARYOTIC DUAL SPECIFICITY TYROSINE PHOSPHORYLATION-REGULATED KINASE (DYRK)-LIKE KINASE *[S]

Received for publication, February 8, 2012, and in revised form, June 14, 2012 Published, JBC Papers in Press, June 18, 2012, DOI 10.1074/jbc.M112.351304

Gunjan Arora[‡1], Andaleeb Sajid[‡1], Mary Diana Arulanandh[‡2], Anshika Singhal[‡1], Abid R. Mattoo[‡], Andrei P. Pomerantsev[§], Stephen H. Leppla[§], Souvik Maiti[‡], and Yogendra Singh[‡3]

From the [‡]Council of Scientific and Industrial Research-Institute of Genomics and Integrative Biology, Mall Road, Delhi 110007, India and the [§]Laboratory of Parasitic Diseases, NIAID, National Institutes of Health, Bethesda, Maryland 20892-3202

Background: Characterization of Ser/Thr protein kinases present in *Bacillus anthracis* genome.
Results: Dual specificity protein kinases were identified, of which one is similar to the eukaryotic DYRK superfamily.
Conclusion: *B. anthracis* has lost key tyrosine kinases and gained novel dual specificity kinases.
Significance: Reporting the first prokaryotic enzyme similar to DYRKs shows that this class of enzymes is not restricted to eukaryotes.

Dual specificity protein kinases (DSPKs) are unique enzymes that can execute multiple functions in the cell, which are otherwise performed exclusively by serine/threonine and tyrosine protein kinases. In this study, we have characterized the protein kinases Bas2152 (PrkD) and Bas2037 (PrkG) from *Bacillus anthracis*. Transcriptional analyses of these kinases showed that they are expressed in all phases of growth. In a serendipitous discovery, both kinases were found to be DSPKs. PrkD was found to be similar to the eukaryotic dual specificity Tyr phosphorylation-regulated kinase class of dual specificity kinases, which autophosphorylates on Ser, Thr, and Tyr residues and phosphorylates Ser and Thr residues on substrates. PrkG was found to be a *bona fide* dual specificity protein kinase that mediates autophosphorylation and substrate phosphorylation on Ser, Thr, and Tyr residues. The sites of phosphorylation in both of the kinases were identified through mass spectrometry. Phosphorylation on Tyr residues regulates the kinase activity of PrkD and PrkG. PrpC, the only known Ser/Thr protein phosphatase, was also found to possess dual specificity. Genistein, a known Tyr kinase inhibitor, was found to inhibit the activities of PrkD and PrkG and affect the growth of *B. anthracis* cells, indicating a possible role of these kinases in cell growth and development. In addition, the glycolytic enzyme pyruvate kinase was found to be phosphorylated by PrkD on Ser and Thr residues but not by PrkG. Thus, this study provides the first evidence of DSPKs in *B. anthracis* that belong to different classes and have different modes of regulation.

The major protein families involved in signal transduction in bacteria are the two-component systems, eukaryotic-like serine/threonine protein kinases (STPKs)[4] and tyrosine kinases (1–3). Eukaryotic-like STPKs regulate diverse functions, such as stress response, growth and development, host-pathogen interactions, and virulence in several pathogenic bacteria (1, 3–8). These STPKs are generally characterized by the presence of 11 Hanks subdomains (9, 10). Bacterial Tyr kinases are autophosphorylating enzymes that regulate virulence, biofilm formation, and DNA replication (11–19). Bacterial Tyr kinases are exclusive P-loop-containing enzymes with Walker motifs for nucleotide binding, such as PtkA of *Bacillus subtilis*, CapB from *Staphylococcus aureus*, and Etk of *Escherichia coli* (19–22). The guanidine phosphotransferase domain-containing enzyme "McsB" of *B. subtilis* was also found to be a Tyr kinase, although its *Bacillus stearothermophilus* homologue is now hypothesized to be an Arg and not Tyr kinase (23, 24). Another unique class of enzymes possess both STPKs and Tyr kinase activities and are recognized as "dual specificity protein kinases" (DSPKs) (25, 26). Although DSPKs are well known in the eukaryotic world, only two have been reported in prokaryotes: PknD of *Chlamydophila pneumoniae* and PutA of *Salmonella typhimurium* (25, 27).

PrkC is the only characterized STPK in *B. anthracis* and *B. subtilis* (28, 29). Recent data showed that the loss of this enzyme (called BA-Stk1) in *B. anthracis* had profound effects on virulence (29, 30). Furthermore, it was found that germinating spores of *B. subtilis* use degraded peptidoglycan fragments

* This work was supported, in whole or in part, by the National Institutes of Health, NIAID, Intramural Research Program. This work was also supported by Council of Scientific and Industrial Research Grant NWP-0038.
[S] This article contains supplemental Tables S1–S3 and Figs. S1–S10.
[1] Senior Research Fellow of the Council of Scientific and Industrial Research, India.
[2] Project assistant of the Council of Scientific and Industrial Research, India.
[3] To whom correspondence may be addressed. Tel.: 11-2766-6156; Fax: 11-2766-7471; E-mail: ysingh@igib.res.in.

[4] The abbreviations used are: STPK, serine/threonine protein kinase; PASTA, penicillin-binding protein and Ser/Thr kinase-associated; RD, Arg-Asp; BLASTp, Basic Local Alignment Search Tool for protein sequences; PAA, phosphoamino acid analysis; 2D-TLE, two-dimensional thin layer electrophoresis; DSPK, dual specificity protein kinase; DYRK, dual specificity Tyr phosphorylation-regulated kinase; MyBP, myelin basic protein; BasPyk, *B. anthracis* pyruvate kinase; TPR, tetratricopeptide repeat; BA-Stk1, *B. anthracis* Ser/Thr kinase 1; BA-Stp1, *B. anthracis* Ser/Thr phosphatase 1; Pyk-P and Pyk-UP, phosphorylated and unphosphorylated BasPyk, respectively.

called "muropeptides" as a germination signal, which is sensed by C-terminal penicillin-binding protein and Ser/Thr kinase-associated (PASTA) domains of PrkC (31). The conformational changes in PrkC after muropeptide binding result in activation of the cytosolic kinase domain, which in turn phosphorylates translation elongation factor Ef-G and aids in germination (31).

Comparative analysis of *B. subtilis* and *B. anthracis* genomes has revealed that whereas the former harbors three Tyr kinases, the latter had only McsB as a representative of the Tyr kinase family (14, 17, 32). It appears that, in comparison with *B. subtilis*, *B. anthracis* has fewer Tyr kinases but more histidine kinases (33). To fully understand the Ser/Thr/Tyr phosphorylation in *B. anthracis*, we sought to identify additional functional STPKs present in *B. anthracis*. *In silico* analysis of the *B. anthracis* genome revealed the presence of four putative STPKs, of which Bas2152 (PrkD) and Bas2037 (PrkG) were similar to the previously characterized BA-Stk1/PrkC (Bas3713), which were studied in detail. In a serendipitous discovery, both the novel kinases (Bas2152 and Bas2037) and the lone Ser/Thr protein phosphatase PrpC (BA-Stp1) were found to have overlapping specificities toward Tyr. Detailed experimental analysis showed that both kinases belong to separate classes of dual specificity protein kinases, with PrkD being the first bacterial "dual specificity tyrosine phosphorylation-regulated kinase" (DYRK). DYRK proteins are defined as dual specificity protein kinases because they can phosphorylate Ser and Thr as well as Tyr residues, although Tyr phosphorylation is restricted to autophosphorylation (34, 35). To date, DYRKs have been shown to exist in eukaryotes but remain elusive in prokaryotes (34). The second enzyme, PrkG, is typical of the DSPK family kinases, which not only autophosphorylate Ser/Thr/Tyr residues but are also capable of phosphorylating their substrates on all three residues (36, 37). The kinase activities of both enzymes were found to be regulated primarily by Tyr phosphorylation. Pyruvate kinase (BasPyk) was identified as a substrate of PrkD, which was phosphorylated on Ser/Thr residues but not on Tyr, thus affirming that PrkD is a DYRK-like kinase.

EXPERIMENTAL PROCEDURES

Bacterial Strains and Growth Conditions—E. coli strain DH5α (Novagen) was used for cloning and BL21 (DE3) (Stratagene) for the expression of recombinant proteins. *E. coli* cells were grown and maintained with constant shaking (220 rpm) at 37 °C in LB broth supplemented with 100 μg/ml ampicillin when needed. *B. anthracis* Sterne strain was grown in LB broth at 37 °C with shaking at 220 rpm. For solid medium, LB-agar was used for both *E. coli* and *B. anthracis*, containing the appropriate antibiotic.

RNA Isolation from B. anthracis and Quantitative Real-time PCR—RNA was isolated from *B. anthracis* Sterne strain cells grown to early log (A_{600} = 0.2–0.3), midlog (A_{600} = 0.8–1.0), late log (A_{600} = 1.5–1.7), and stationary phases (A_{600} >2.2, ~30 h), using the protocols described previously with some modifications (38–40). To isolate RNA, cells were centrifuged at 6,000 × *g* for 15 min and resuspended in 400 μl of hot lysis buffer (50 mM Tris (pH 8.0), 1 mM EDTA, and 1% SDS) kept at 65 °C followed by incubation with lysozyme (0.25 mg/ml) at 37 °C for 10 min. Lysis was carried out by transferring the suspension to 1.5-ml vials containing 400 μl of acidified glass beads (425–600 nm; Sigma) and 500 μl of phenol kept at 65 °C. This was followed by incubation at 65 °C for 15 min with vortexing for 30 s after every 5 min. The upper aqueous phase containing RNA was then separated by centrifugation at 9,500 × *g* for 15 min at 4 °C, to which equal volumes of TRIzol® (Invitrogen) and 100 μl of chloroform/ml of TRIzol was added, mixed well, and centrifuged at 9,500 × *g* for 15 min at 4 °C. RNA from the upper aqueous phase was then precipitated with $LiCl_2$ (0.5 M final) and three volumes of ice-cold isopropyl alcohol followed by incubation at −80 °C for 2 h and centrifugation at 16,000 × *g* for 20 min at 4 °C. The pellet was then washed with 70% ethanol, and the air-dried pellet was dissolved in 20 μl of nuclease-free water and stored at −80 °C.

Before performing cDNA synthesis, RNA was treated with DNase (Ambion) according to the manufacturer's protocol to remove the traces of genomic DNA. cDNA was made from 400 ng of RNA of each phase, according to the protocol provided by the supplier (Applied Biosystems), which was then used for checking the expression of the gene with gene-specific primers. For quantitative real-time PCR, a standard curve was prepared using serial dilutions of the kinase clone for the corresponding kinase gene in different copy numbers (copy numbers 10^1, 10^2, 10^3, 10^4, 10^5, and 10^6). Real-time PCR was performed using SYBR Green master mix according to the manufacturer's instructions. For the standard curve, reactions were run in triplicates, under the same conditions and using the same primers as that for the kinase genes. For expression analysis, 1 μl of cDNA (each phase) was used in a 15-μl PCR, in duplicates, together with no template controls. The *fusA* gene, which encodes translation elongation factor G, was used as an external control (41). All primers were sequence-specific for each gene analyzed, with PCR products between 70 and 100 bp.

Gene Manipulation—For cloning of $PrkC_c$ (*bas3713*, the cytosolic region of amino acids 1–337), PrkD (*bas2152*), PrkG (*bas2037*), PrpC (*bas3714*), and BasPyk (*bas4492*), the genes were PCR-amplified from *B. anthracis* genomic DNA using gene-specific forward and reverse primers. The resulting PCR products were then digested and cloned into the BamHI and XhoI sites of pProEx-HTc (Invitrogen) and/or pGEX-5X-3 (GE Healthcare) vectors previously digested with the same enzymes. The clones were confirmed with restriction digestion and DNA sequencing (TCGA, New Delhi, India). The details of primers and plasmids are provided in supplemental Table S1.

To generate essential lysine mutants and phosphorylation site derivatives of both kinases, site-directed mutagenesis was carried out using the QuikChange® XL site-directed mutagenesis kit (Stratagene) as per the manufacturer's instructions, using HTc-PrkD and HTc-PrkG as templates. The clones were confirmed with DNA sequencing (TCGA).

Protein Expression and Purification—The recombinant plasmids were transformed and overexpressed in *E. coli* BL-21 (DE3) cells. The proteins were purified by Ni^{2+}-NTA or glutathione-Sepharose affinity columns (Qiagen) as described earlier (42). The purified proteins were visualized by 10–15% SDS-PAGE, and the concentrations were estimated by a Bradford assay (Bio-Rad).

Immunoblotting Analysis—To detect the phosphorylated residues of PrkD and PrkG, proteins were resolved by SDS-PAGE and transferred onto a nitrocellulose membrane. Blots were then blocked with 3% bovine serum albumin in phosphate-buffered saline containing 0.1% Tween 20 (PBST) overnight at 4 °C. This was followed by incubation with primary antibodies anti-Tyr(P) (Upstate Biotechnology) and anti-Ser(P)/Thr(P) (Invitrogen) at 1:10,000 dilution and goat anti-rabbit IgG secondary antibodies (Bangalore Genei) (1:10,000) for 1 h each at room temperature. The blots were developed using the SuperSignal® West Pico Chemiluminescent Substrate kit (Pierce) according to the manufacturer's instructions. Autophosphorylated PrkC was kept as a negative control for the α-Tyr(P) blot because it has been reported to be phosphorylated on Ser and Thr residues (30). Phosphorylated myelin basic protein (MyBP) phosphorylated by the Tyr kinase Abl (New England Biolabs) was used as a positive control.

Generation of Polyclonal Antibodies against PrkG in Rabbits and Verification of PrkG Expression—Purified His_6-PrkG protein (400 μg) was emulsified in Freund's complete adjuvant (1:1 ratio) and injected into rabbits. Subsequently, injections of 400 μg each of His_6-PrkG in 1 ml of Freund's incomplete adjuvant were given three times at 21-day intervals. Fourteen days after the final injection, animals were bled, and titers of anti-His_6-PrkG were determined by ELISA as described previously by Koul *et al.* (43). The molecular weight of PrkG was verified using 40 μg of *B. anthracis* whole cell lysate. The lysate was resolved by SDS-PAGE along with suitable positive (His_6-PrkG (1 μg)) and negative (glutathione *S*-transferase (2 μg)) controls. Proteins were transferred onto nitrocellulose membrane (Bio-Rad), and a standard procedure for immunoblotting was followed using 1:20,000 dilutions of primary and secondary antibodies, as described under "Immunoblotting Analysis."

In Vitro Kinase and Phosphatase Assays—In vitro phosphorylation assays of 25 pmol of $PrkC_c$, PrkD, and PrkG or their derivatives were carried out in kinase buffer (20 mM HEPES (pH 7.2), 1 mM DTT, 5 mM $MgCl_2$, and 5 mM $MnCl_2$ for all of the kinases) containing 2 μCi of [γ-^{32}P]ATP (Board of Radiation and Isotope Technology, Hyderabad, India) followed by incubation at 25 °C for 20 min. The ionic requirement was estimated by *in vitro* kinase assays with 25 pmol of kinase in 20 mM HEPES (pH 7.2) and 1 mM DTT, together with either metal ion ($MgCl_2$/$MnCl_2$) and 2 μCi of [γ-^{32}P]ATP. Nucleotide specificity assays of PrkD and PrkG were performed similarly by using 2 μCi of [γ-^{32}P]ATP or [γ-^{32}P]GTP (Board of Radiation and Isotope Technology). For substrate phosphorylation, 5 μg of MyBP and 2–5 μg of BasPyk were used. Proteins were separated by 10–15% SDS-PAGE and analyzed by a PhosphorImager (FLA 2000, Fuji).

In vitro dephosphorylation assays were carried out by adding PrpC (~35 pmol) to the reactions after kinase assays, followed by additional incubation for different times up to 30 min at 37 °C, as also described by Sajid *et al.* (44). Reactions were terminated by 5× SDS sample buffer followed by boiling at 100 °C for 5 min. Proteins were separated by 10–15% SDS-PAGE and analyzed by a PhosphorImager.

To check the phosphatase specificity, non-radioactive P_i release assays were performed. The sequence of phosphopeptides (Millipore) that were used in the assay was as follows: KRpTIRR (catalog no. 12-219), RRApSVA (catalog no. 12-220), and RRLIEDAEpYAARG (catalog no. 12-217). The assays were performed according to the instructions provided in the manual Ser/Thr phosphatase assay system by Promega.

Kinase Inhibition Assays—For inhibition assays, the specified inhibitor (Calbiochem and Sigma) was added in the concentration gradient in the kinase buffer. In the resultant mixture, PrkD/PrkG (25 pmol) was added, and further *in vitro* kinase assays were carried out as discussed before. The control reactions contained DMSO (solvent in which inhibitors were dissolved).

Construction of B. anthracis mcsB Deletion Strain (BasΔmcsB)—The Cre-*loxP* genetic modification method was used to introduce precise genetic knockouts into the *B. anthracis* gene encoding McsB as previously discussed in detail by Pomerantsev *et al.* (45). Precisely, the pSC vector was used to produce a deletion of region (800 bases deleted of a total of 1062 nucleotides of *mcsB*) in two-step recombination using the primer pair sequence provided in supplemental Table S1. Plasmid pCrePAS was used for elimination of DNA regions containing a spectinomycin resistance cassette located between two similarly oriented *loxP* sites. The deletion of the *mcsB* gene in the BasΔ*mcsB* strain was confirmed by PCR and DNA sequencing.

B. anthracis Growth Inhibition—B. anthracis primary culture was inoculated from a single colony on an LB agar plate and grown until reaching an A_{600} of 1.0. Secondary cultures were then inoculated from the primary culture (0.1%). To study the effect of genistein, cultures were grown in the presence of 20 and 100 μM, in duplicate. Absorbance was measured at 600 nm and plotted against time.

Phosphoamino Acid (PAA) Analysis—For this analysis, 100 pmol of autophosphorylated ^{32}P-PrkD and ^{32}P-PrkG was separated by SDS-PAGE after an *in vitro* kinase assay and electroblotted onto Immobilon PVDF membrane (Millipore). PAA analysis by two-dimensional thin layer electrophoresis (2D-TLE) was performed as described previously (46). After 2D-TLE, the plate was dried and sprayed with 1.0% ninhydrin. The plate was kept at 55 °C for 15 min, and three spots corresponding to Ser(P), Thr(P), and Tyr(P) were observed. The plate was kept for exposure under x-ray for 3–4 days. The autoradiogram was analyzed by overlapping the corresponding TLC plate to identify the radiolabeled Ser(P)/Thr(P)/Tyr(P) residues. Substrates ^{32}P-MyBP (phosphorylated by PrkD or PrkG) and ^{32}P-BasPyk (phosphorylated by PrkD) were also similarly analyzed.

Identification of Phosphorylation Sites—For protein analysis by mass spectrometry, a Coomassie-stained protein band was cut from a polyacrylamide gel and digested with trypsin as described previously (47). Proteolytic fragments were analyzed by LC-MS/MS with electrospray ionization using an Applied Biosystems 5600 Triple-TOF mass spectrometer (AB-Sciex, Toronto, Canada). Interpretation of spectra was performed manually with the aid of Protein Prospector software (University of California, San Francisco).

Pyruvate Kinase (bas4492) Cloning in pET-Duet1 Vector and Analysis of Phosphorylation—For co-expression studies, the dual expression vector pET-Duet1 (Novagen) was used, as described previously by Khan *et al.* (48, 49). For cloning in pET-Duet-1, the gene coding for BasPyk (*bas4492*) was cloned in

TABLE 1
Differences between PrkD and PrkG

Characteristic	PrkD	PrkG
Expression analysis	All phases, maximum in late log phase, less than PrkG except in stationary phase	All phases, maximum in mid- and late-log phases
Hanks subdomains	10	7
Activation loop	Present, RD kinase	Absent, non-RD kinase
Dual specificity/class	Yes/DYRK	Yes/DSPK
Autophosphorylation	Ser/Thr/Tyr	Ser/Thr/Tyr
Transphosphorylation	Ser/Thr	Ser/Thr/Tyr
Involvement of Tyr	Autophosphorylation and substrate phosphorylation	Autophosphorylation
Conservation	Throughout *Bacillus* species	Only in pathogenic *B. cereus* group
Rossmann fold	Present	Irregular
Substrate phosphorylation		
MyBP	Yes	Yes
BasPyk	Yes	No

MCS1 having an N-terminal His_6 tag. In MCS2 of pETDuet-1-His_6-BasPyk, either the PrkD or its catalytically inactive mutant $PrkD^{K53M}$ was subcloned using HTc-PrkD and HTc-$PrkD^{K53M}$ as templates and an appropriate primer pair. The primer sequences with restriction sites are provided in supplemental Table S1. The two plasmids pETDuet-1-His_6-BasPyk-PrkD and pETDuet-1-His_6-BasPyk-$PrkD^{K53M}$ were transformed in *E. coli* BL21 cells. The phosphorylated BasPyk (Pyk-P) and unphosphorylated BasPyk (Pyk-UP) were purified from cells overexpressing pETDuet-1-His_6-BasPyk-PrkD and pETDuet-1-His_6-BasPyk-$PrkD^{K53M}$, respectively, using Ni^{2+}-NTA-Sepharose columns. The phosphorylation status of Pyk-P and Pyk-UP was detected by Pro-Q® Diamond phosphoprotein gel stain (Molecular Probes, Invitrogen) and later compared with SYPRO® Ruby protein gel stain (Molecular Probes, Invitrogen) according to the manufacturer's instructions and analyzed by a Typhoon trio variable mode analyzer (GE Healthcare).

Enzymatic Assay of BasPyk and Determination of Kinetic Parameters—Pyruvate kinase activity was determined at 37 °C by the coupled lactate dehydrogenase assay as described previously (50, 51) except for some modifications. The reaction mixture (100 μl) contained 100 mM Tris-HCl buffer (pH 7.4), 10 mM $MgCl_2$, 1 mM NADH (Sigma), 20 mM ADP (Sigma), pH 7.2, 1–8 mM phosphoenolpyruvate (Sigma) and 15 μg of lactate dehydrogenase (Sigma). The reaction was started by the addition of 10 nM enzyme. The reaction was performed for 10 min, and absorbance was measured at 340 nm (Bio-Rad Microplate reader 680 XR). K_m and V_{max} values were determined by nonlinear regression analyses (curve fit) using GraphPad Prism software. Data (specific activity) from three independent experiments were plotted, and results are presented as average values ± S.D.

RESULTS

In Silico Analysis of B. anthracis STPKs—To identify Ser/Thr protein kinases, a BLASTp search (with default settings) was performed in the *B. anthracis* Sterne strain non-redundant protein sequence database (NCBI, National Institutes of Health) using the sequence of BASPrkC. We identified two genes, *bas2152* (named PrkD) and *bas2037* (named PrkG), which apparently encode Ser/Thr protein kinases. Additionally, two other STPK-encoding genes were also identified as *bas2464* and *bas2527* by pkinase software (pfam). Sequence analysis also revealed that *B. anthracis* has five putative STPK-encoding genes, whereas *B. subtilis* has four such putative STPK-encoding genes (supplemental Table S2).

Although PrkC and its homologs are known to be activated through C-terminal sensor PASTA domains, PrkD and PrkG seem to only possess N-terminal kinase domains, as suggested by SMART domain analysis (supplemental Fig. S1). Alignment of catalytic domain sequences of both PrkD and PrkG with PrkC revealed that all 12 signature motifs, which are characteristic of their eukaryotic counterparts, are more conserved in PrkD in comparison with PrkG (Table 1 and supplemental Fig. S2). The main differences were found in conserved catalytic Arg and Asp residues, which divide these kinases into RD and non-RD classes (52, 53). PrkD is an RD kinase, and therefore phosphorylation of the activation loop residues governs its activity. PrkG belongs to the non-RD kinase class with no activation loop. Other key differences between the two kinases are shown in Table 1.

To identify homologs of these kinases in other *Bacillus* species, a BLASTp search was performed using the protein sequences of PrkD and PrkG. The results indicated that PrkD homologs are conserved in the *Bacillus* species (Fig. 1*A*), whereas PrkG is unique to the pathogenic *Bacillus cereus* group (Fig. 1*B* and Table 1). PrkG homologs in the *B. cereus* group have tetratricopeptide repeat (TPR) domains at the C terminus in addition to the kinase domain. Therefore, in order to understand the differences in domain organization, flanking genes of PrkG were also compared with their homologs. It was found that the kinase domain (Bas2037) and TPR domain (Bas2038) exist as two separate proteins in most *B. anthracis* strains sequenced so far (*B. anthracis* strains A1055, A0442, A0465, CNEVA-9066, and Kruger B being the only exceptions) but not in other *B. cereus* group species. A nonsense mutation in most *B. anthracis* strains resulted in a stop codon (Fig. 1*B*), and therefore a truncated form of the kinase is expressed in the bacterium, as confirmed by immunoblotting with polyclonal antibodies against PrkG (supplemental Fig. S3).

Expression of B. anthracis Kinases during Different Growth Phases—The presence of multiple kinase-encoding ORFs in the *B. anthracis* genome intrigued us to define their transcriptional pattern and to determine the general expression profiles. We quantified the transcript number of each of the three kinase genes by quantitative real-time PCR and found variation in expression of these regulatory enzymes in various stages of growth (Fig. 1*C*). The *bas3713* (*prkC*) was consistently expressed in early log (A_{600} = 0.2–0.3), midlog (A_{600} = 0.8–1.0), and late log (A_{600} = 1.5–1.7) phases, whereas the expression decreased in stationary phase (A_{600} > 2.2, ~30 h). The

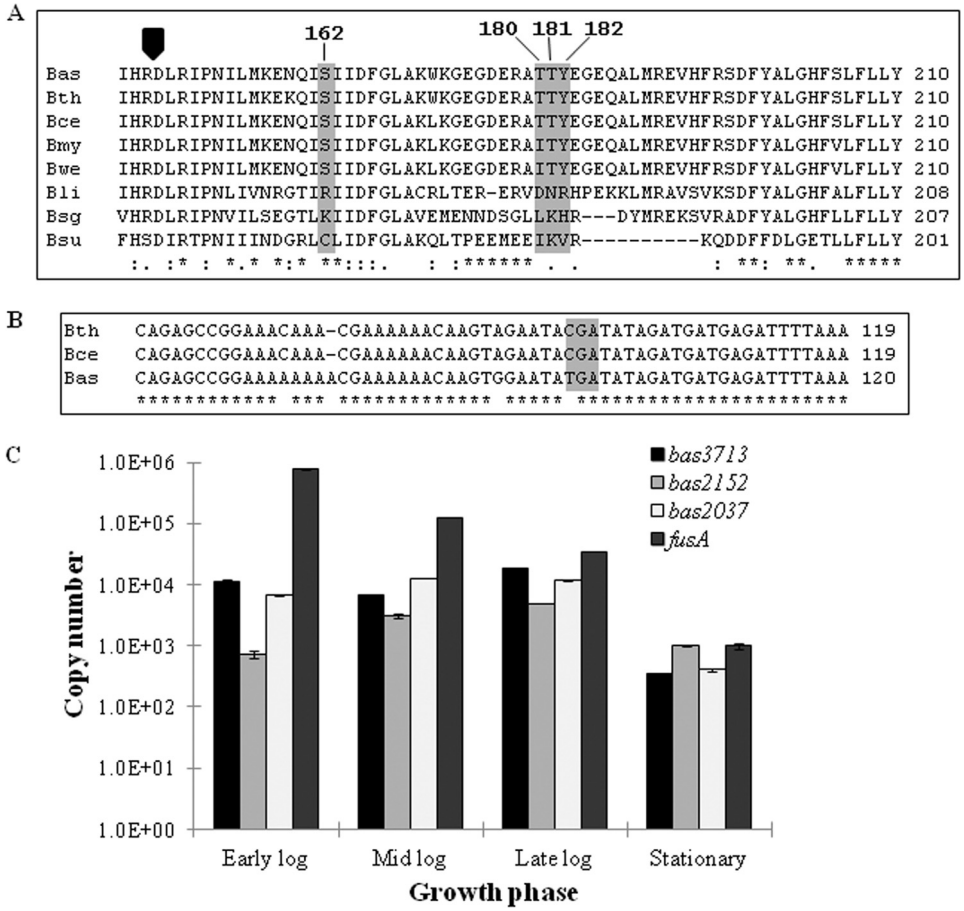

FIGURE 1. **Bioinformatic and expression analysis of PrkD and PrkG.** *A*, multiple sequence alignment of PrkD with its homologs from other *Bacillus* species. The conserved RD sequence is marked by a *black arrow*. The TTY sequence in the activation loop and Ser^{162} are *highlighted* and shown in the *box*. The species chosen are *B. anthracis* Sterne strain (*Bas*), *B. thuringiensis* serovar *andalousiensis* BGSC 4AW1 (*Bth*), *B. cereus* E33L (*Bce*), *Bacillus mycoides* DSM 2048 (*Bmy*), *Bacillus weihenstephanensis* KBAB4 (*Bwe*), *Bacillus licheniformis* ATCC 14580 (*Bli*), *Bacillus* sp. SG-1 (*Bsg*), and *B. subtilis* (*Bsu*). *B*, multiple sequence alignment of *bas2037* (*prkG*) gene with its homologs in the *B. cereus* group, with the stop codon shown in a *gray box*. The species chosen are *B. thuringiensis* serovar *andalousiensis* BGSC 4AW1 (*Bth*), *B. cereus* E33L (*Bce*), and *B. anthracis* Sterne strain (*Bas*). *C*, expression analysis of *B. anthracis* STPKs by quantitative real-time PCR performed with RNA isolated from *B. anthracis* vegetative cells in different growth phases. The *fusA* was used as a control gene. The *graph* shows logarithmic scale of copy number *versus* growth phase. The experiment was performed in triplicate, and the *error bars* represent S.D. of three individual readings.

expression of *bas2152* (*prkD*) was lower than that of *bas3713* in all growth phases, except in stationary phase, where it was approximately 3 times more abundant than *bas3713*. Transcripts of *bas2037* were also present in all four stages, and expression was comparable with *bas3713*, with the exception of the midlog phase, where *bas2037* was almost 2-fold more abundant than *bas3713*. Copy number was calculated by constructing a standard curve using a known plasmid with the same gene as the standard. Translational enzyme elongation factor G (*fusA*) was used as an external control, whose expression was higher than all kinases in all growth phases except for stationary phase (Fig. 1*C*). This expression profile of *fusA* corroborates with earlier reports (41, 54), where it has been used as an external control and a similar expression profile has been shown. These data indicate that all of the kinases are expressed during the growth cycle, albeit at different levels.

Biochemical Characterization of PrkD and PrkG—Signal transduction proteins, such as kinases, play an important role in the adaptation of living organisms to changing environments (2). Therefore, it is crucial to elucidate their regulation. In order to characterize these kinases, the genes coding PrkD and PrkG were cloned, overexpressed, and purified from *E. coli* as His_6 tag fusion proteins. To analyze their nucleotide specificity and ionic requirements, *in vitro* kinase assays were performed with either [γ-^{32}P]ATP or [γ-^{32}P]GTP in the presence of different divalent ions. Proteins were resolved by SDS-PAGE and then analyzed on an autoradiogram for comparison of phosphorylation signal by quantification with ImageGauge software (Fuji). Both kinases were found to be ATP-dependent and required Mg^{2+} or Mn^{2+} ions for activity (Fig. 2*A*). Under the conditions tested, both kinases were found to be maximally active at 25 °C (Fig. 2*B* and supplemental Fig. S4*A*). Therefore, all further assays were performed at 25 °C in the presence of Mg^{2+} and Mn^{2+}. Furthermore, time-dependent phosphorylation assays were performed to calculate the activation time for these kinases. Although both PrkD and PrkG were able to autophosphorylate within 1 min, optimal phosphorylation was achieved within 5 min (Fig. 2*C* and supplemental Fig. S4*B*).

Identification of Autophosphorylation Sites in PrkD and PrkG—Most STPKs exhibit autophosphorylation at multiple sites, the loss of which may impair the kinase activity. Therefore, PAA analysis of PrkD and PrkG was performed after an *in vitro* kinase assay by 2D-TLE to identify the phosphorylated residue(s). Interestingly, both kinases were found to be phosphor-

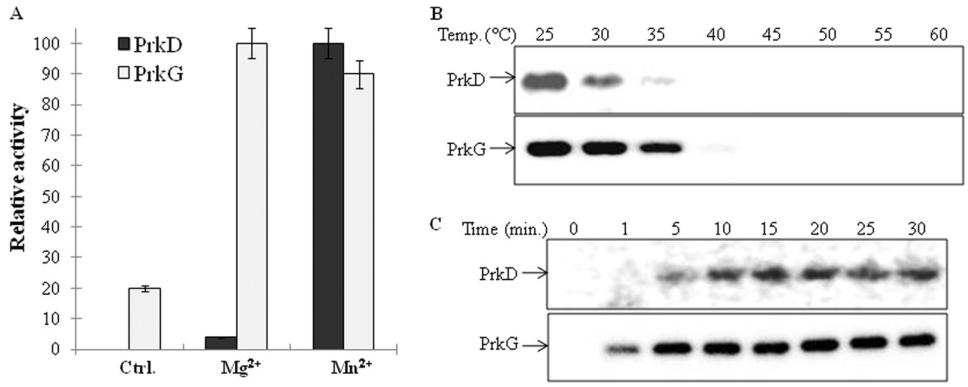

FIGURE 2. **Biochemical characterization of PrkD and PrkG.** *A*, activation of PrkD and PrkG by Mg^{2+} and Mn^{2+} was assessed by *in vitro* kinase assays followed by autoradiography. The bands were quantitated by ImageGauge software. Maximum activity of PrkD was observed in the presence of Mn^{2+}, which was taken as 100% and used to calculate the relative phosphorylation. The maximum activity of PrkG was observed in the presence of Mg^{2+}, which was taken as 100% and used to calculate relative phosphorylation. Activity in the absence of any added ion was used as a control. The experiment was performed three times, and the *error bars* represent S.E. of three individual values. *B*, autoradiograms showing the temperature-dependent activation of PrkD (*top*) and PrkG (*bottom*). Maximum activity of both kinases was observed at 25 °C. The corresponding SDS-PAGE is shown in supplemental Fig. S4*A*. *C*, autoradiograms showing time-dependent phosphorylation of PrkD (*top*) and PrkG (*bottom*). The corresponding SDS-PAGE is shown in supplemental Fig. S4*B*.

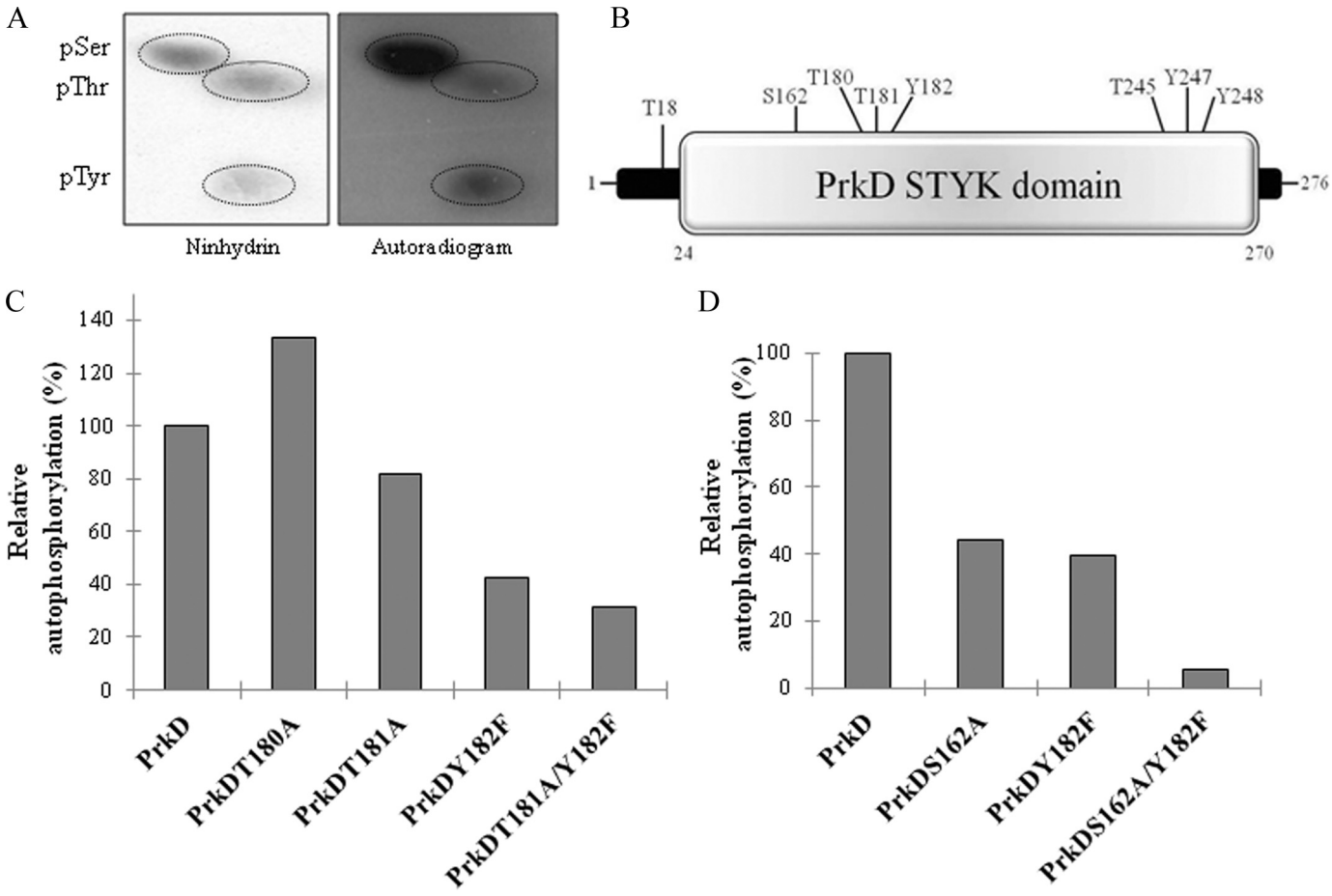

FIGURE 3. **Analysis of phosphorylated residues of PrkD.** *A*, PAA analysis of autophosphorylated PrkD by 2D-TLE. *Left*, ninhydrin-stained TLC plate; *right*, corresponding autoradiogram. The phosphoresidues are *circled*. *pSer*, *pThr*, and *pTyr*, phospho-Ser, -Thr, and -Tyr, respectively. *B*, diagram showing the phosphorylated residues in the PrkD STYK domain (SMART domain analysis) as Thr^{18}, Ser^{162}, Thr^{180}, Thr^{181}, Tyr^{182}, Thr^{245}, Tyr^{247}, and Tyr^{248}. *C* and *D*, mutants of phosphorylated residues in the activation loop of PrkD were assessed for loss of a phosphorylation signal. *In vitro* kinase assays were performed followed by autoradiography and analyzed by ImageGauge software. Phosphorylation of wild-type PrkD was taken as 100% and used to calculate the relative phosphorylation. Each experiment was repeated three times with fresh purification lots of the kinase and its derivatives. The corresponding SDS-PAGE and autoradiogram are shown in supplemental Fig. S6, *A* and *B*.

ylated on Tyr residues in addition to Ser and Thr (Figs. 3*A* and 4*A*). This was further confirmed by immunoblotting with α-Tyr(P) antibodies (supplemental Fig. S5) as well as α-Ser(P) and α-Thr(P) antibodies (data not shown).

To prove this distinctive nature of PrkD and PrkG, it was pertinent to determine the sites of phosphorylation. Mass spectrometry analysis of PrkD identified several phosphorylated Ser/Thr residues and three Tyr residues (Fig. 3*B*). Of these, one

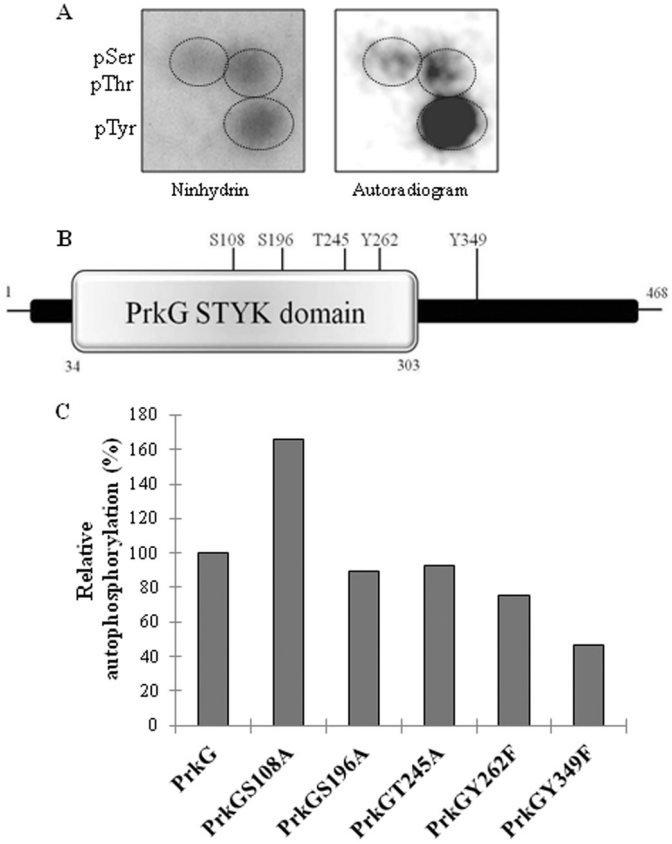

FIGURE 4. **Analysis of phosphorylated residues of PrkG.** *A*, PAA analysis of autophosphorylated PrkG. *Left*, ninhydrin-stained TLC plate; *right*, corresponding autoradiogram. *pSer*, *pThr*, and *pTyr*, phospho-Ser, -Thr, and -Tyr, respectively. *B*, diagram showing the phosphorylated residues of PrkG as Ser^{108}, Ser^{196}, Thr^{245}, Tyr^{262}, and Tyr^{349}. *C*, mutants of phosphorylated residues in the activation loop of PrkG were assessed for loss of phosphorylation signal. Phosphorylation of wild-type PrkG was taken as 100% and used to calculate the relative phosphorylation. The corresponding SDS-PAGE and autoradiogram are shown in supplemental Fig. S6*C*.

phosphorylated residue (Tyr^{182}) and two probable phosphoresidues (Thr^{180} and Thr^{181}) were present in the activation loop of the PrkD catalytic domain. A multiple sequence alignment of the activation loop of PrkD and its homologs revealed that Tyr^{182} is conserved only in the pathogenic *B. cereus* group (Fig. 1*A*). Therefore, to study the impact of Tyr phosphorylation on kinase activation and to gain a better understanding of its effect on the phosphorylation of PrkD, all three residues were mutated to generate single mutants $PrkD^{T180A}$, $PrkD^{T181A}$, and $PrkD^{Y182F}$ as well as the $PrkD^{T181A/Y182F}$ double mutant. Equal amounts of PrkD and its mutants were used in the *in vitro* kinase assays with [γ-^{32}P]ATP, resolved by SDS-PAGE, and then analyzed on an autoradiogram for loss of phosphorylation signal by quantification with ImageGauge software. The analysis indicated that maximum loss in activity was observed in the $PrkD^{Y182F}$ mutant (Fig. 3*C* and supplemental Fig. S6*A*), suggesting that this site is central for PrkD activation. The $PrkD^{T181A}$ mutant also exhibited a loss in signal, and the importance of Thr^{181} and Tyr^{182} was also confirmed by generating the double mutant $PrkD^{T181A/Y182F}$, which showed ~70% loss in phosphosignal. These results indicate that the two major phosphorylation sites in the PrkD activation loop are Thr^{181} and Tyr^{182}. Interestingly, $PrkD^{T180A}$ showed hyperphosphorylation, which indicates that it may not be phosphorylated and may only have an accessory role in controlling the phosphorylation within the activation loop. The importance of Tyr^{182} was reflected by minor loss of kinase activity between the $PrkD^{T180A/T181A}$ mutant and PrkD. Furthermore, to find the effect of Ser^{162}, the only phosphorylated Ser residue present adjacent to the activation loop, we also generated $PrkD^{S162A}$ and $PrkD^{S162A/Y182F}$ mutants. Both mutants showed loss in autophosphorylation activity compared with PrkD, with more prominent losses exhibited by $PrkD^{S162A/Y182F}$ (Fig. 3*D* and supplemental Fig. S6*B*) Together, these results suggest that PrkD is a dual specificity kinase.

Mass spectrometry analysis of PrkG also verified it to be a dual specificity kinase, which autophosphorylates at Ser, Thr, and Tyr residues. In PrkG, the phosphorylation sites are scattered throughout the protein as Ser^{108}, Ser^{196}, Thr^{245}, Tyr^{262}, and Tyr^{349} (Fig. 4*B*). Because there is no activation loop present in this kinase, the contribution of all of these sites to PrkG activation was individually assessed. Site-directed mutagenesis was performed to create $PrkG^{S108A}$, $PrkG^{S196A}$, $PrkG^{T245A}$, $PrkG^{Y262F}$, and $PrkG^{Y349F}$ mutants, and the kinase activity of these mutants was compared with native PrkG. As shown in Fig. 4*C* and supplemental Fig. S6*C*, $PrkG^{Y349F}$ showed the maximum loss of phosphorylation compared with the other mutants. For the other mutants, minor losses were observed, with the exception of $PrkG^{S108A}$, which was hyperphosphorylated compared with native PrkG. These results suggest that Tyr^{349} is the major residue that regulates autophosphorylation of PrkG.

Substrate Phosphorylation Mechanisms of PrkD and PrkG—An understanding of the substrate phosphorylation mechanisms of these enzymes was necessary for further investigation of their nature. Phosphorylation of the nonspecific kinase substrate MyBP demonstrated that PrkD and PrkG are capable of substrate phosphorylation (Figs. 5*A* and 6*A*). Based on the sequence homology with *Mycobacterium tuberculosis* PknB and *B. anthracis* PrkC, the invariant Lys residues in subdomain II, essential for catalytic activity, were identified as Lys^{53} of PrkD and Lys^{57} of PrkG (29, 42) (supplemental Fig. S2). Mutations of $PrkD^{K53M}$ and $PrkG^{K57M}$ resulted in complete loss of autokinase activity and phosphorylation on MyBP (Figs. 5*A* and 6*A*). MyBP was found to be advantageous as a common substrate and was further employed to study the role of PrkD- and PrkG-mediated phosphorylation of substrates.

PAA analysis of PrkD-dependent phosphorylation on MyBP showed that only Ser and Thr residues were phosphorylated, but no signal was observed that corresponded to Tyr(P) (Fig. 5*B*). This feature strikingly resembles the DYRK class. To check the effect of PrkD mutations on substrate phosphorylation activity of PrkD, we compared the phosphorylation of MyBP substrate. We found that PrkD Ser^{162}, Thr^{181}, and Tyr^{182} residues were required for efficient substrate phosphorylation, with Tyr^{182} having the strongest effect between the three residues (Fig. 5, *C* and *D*, and supplemental Fig. S6, *D* and *E*).

To understand the role of Tyr phosphorylation in PrkG, the status of substrate phosphorylation was studied. PAA analysis demonstrated that MyBP was phosphorylated on Ser, Thr, and Tyr residues by PrkG (Fig. 6*B*). The substrate phosphorylation

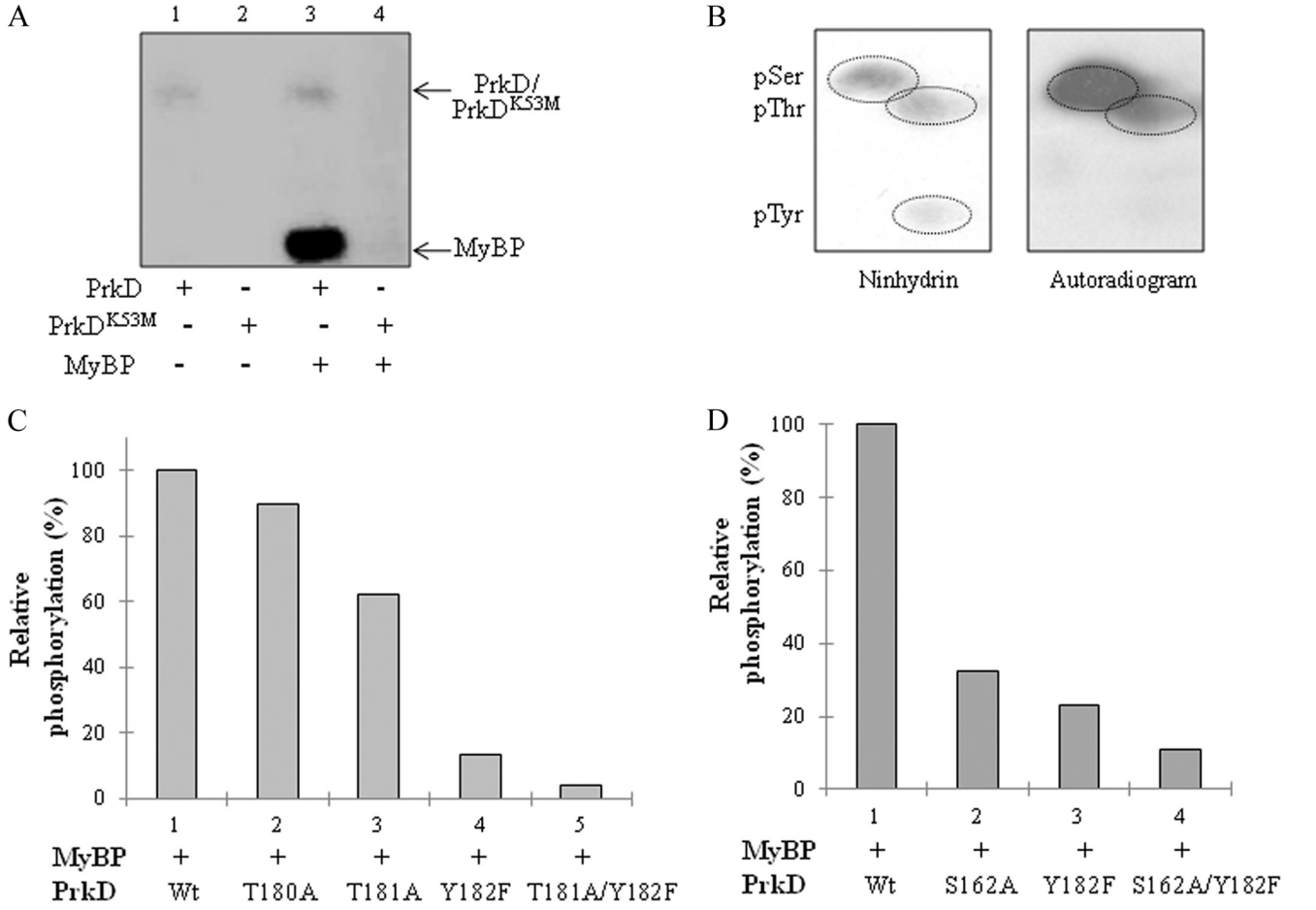

FIGURE 5. **Phosphorylation of MyBP by PrkD.** *A*, *in vitro* kinase assays of PrkD and PrkD^{K53M} with the MyBP substrate. The autoradiogram shows PrkD alone (*lane 1*), PrkD^{K53M} alone (*lane 2*), PrkD with MyBP (*lane 3*), and PrkD^{K53M} with MyBP (*lane 4*). As shown in the autoradiogram, no phosphorylation was observed when the PrkD^{K53M} mutant was used in the assay. *B*, PAA analysis of MyBP phosphorylated by PrkD. *Left*, ninhydrin-stained TLC plate; *right*, corresponding autoradiogram marked with ^{32}P-labeled phosphoresidues. *pSer*, *pThr*, and *pTyr*, phospho-Ser, -Thr, and -Tyr, respectively. *C* and *D*, histograms showing the effect of PrkD and its derivatives on substrate phosphorylation on MyBP. The phosphorylation signal of MyBP by wild-type PrkD (*Wt*) was taken as 100%, and the relative phosphorylation was calculated by ImageGauge software. The corresponding SDS-PAGE and autoradiogram are shown in supplemental Fig. S6, *D* and *E*.

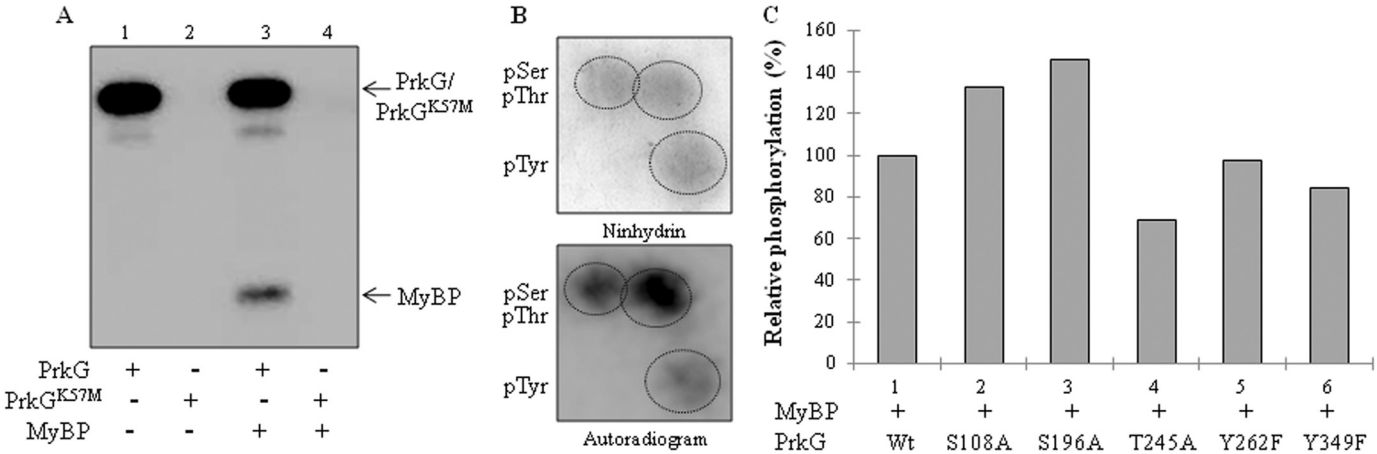

FIGURE 6. **Phosphorylation of MyBP by PrkG.** *A*, *in vitro* kinase assays of PrkG and PrkG^{K57M} with MyBP. The autoradiogram shows PrkG alone (*lane 1*), PrkG^{K57M} alone (*lane 2*), PrkG with MyBP (*lane 3*), and PrkG^{K57M} with MyBP (*lane 4*). No phosphorylation was observed when the kinase-dead mutant PrkG^{K57M} was used in the assay. *B*, PAA analysis of MyBP phosphorylated by PrkG. *Top*, ninhydrin-stained TLC plate; *bottom*, corresponding autoradiogram marked with ^{32}P-labeled phosphoresidues. *pSer*, *pThr*, and *pTyr*, phospho-Ser, -Thr, and -Tyr, respectively. *C*, histogram comparing the effect of phosphorylation site mutations on PrkG-mediated phosphorylation on MyBP. The phosphorylation signal on MyBP by wild-type PrkG (*Wt*) was taken as 100%, and the relative phosphorylation was calculated by ImageGauge software. The corresponding SDS-PAGE and autoradiogram are shown in supplemental Fig. S6*F*.

ability of the PrkG phosphorylation site mutants was also assessed, and interestingly, the PrkG^{T245A} and PrkG^{Y349F} mutants had the greatest impairment in phosphorylation of MyBP (Fig. 6*C* and supplemental Fig. S6*F*). The role of Thr^{245} and Tyr^{349} was further verified by mutating multiple phosphorylation sites in PrkG in combination (data not shown). This

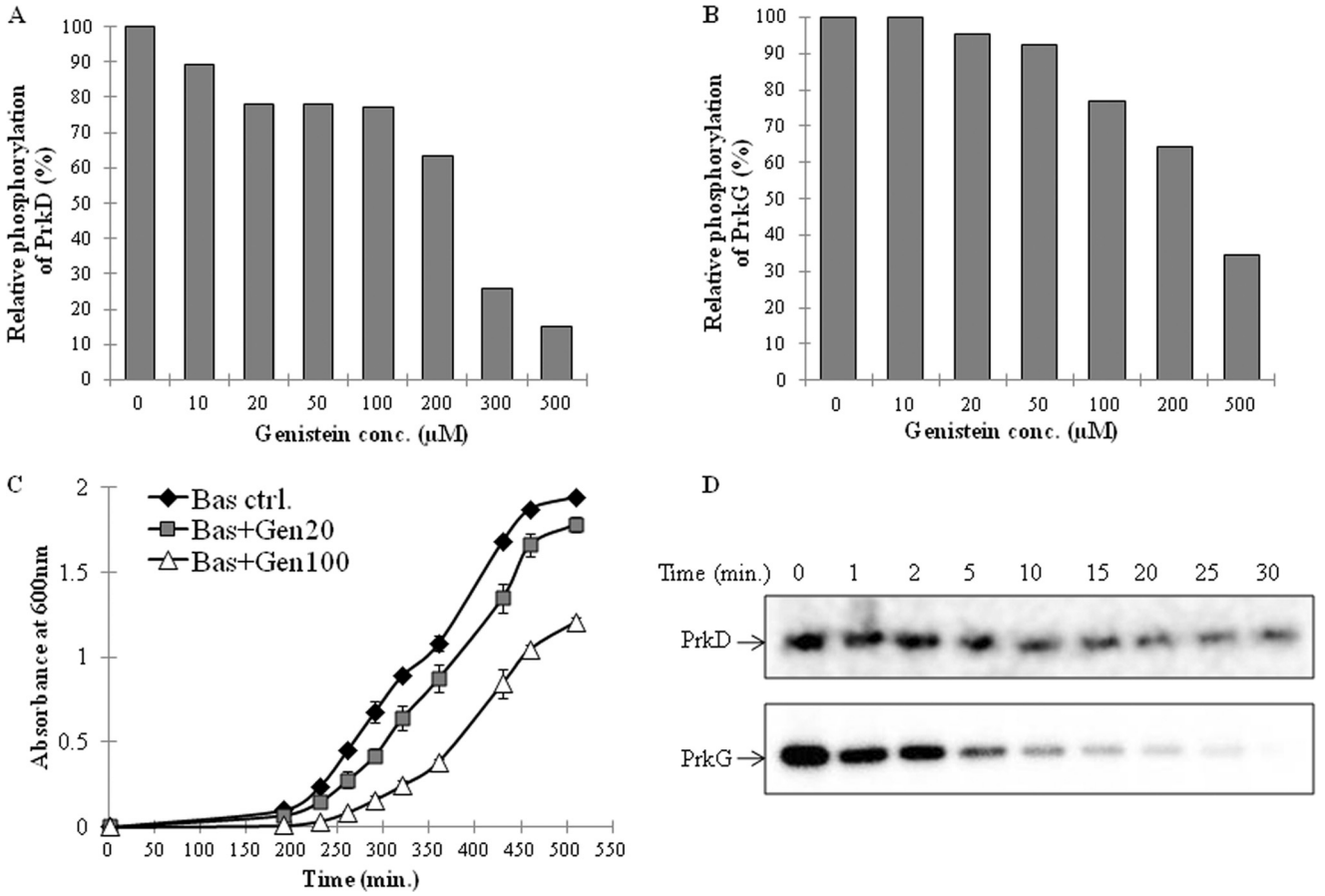

FIGURE 7. **Inhibition of PrkD and PrkG by genistein and its effect on cell growth.** *In vitro* kinase assays were performed with PrkD (*A*) and PrkG (*B*), in the presence of increasing genistein concentrations. The signal intensity with DMSO (vehicle) and without any inhibitor was taken as 100% and used to calculate the relative loss. The corresponding SDS-PAGE and autoradiogram are shown in supplemental Fig. S7, *A* and *B*. *C*, growth curve analysis of *B. anthracis* Sterne strain in the absence (*black diamond*) and presence of genistein (20 μM (*gray square*) and 100 μM (*white triangle*). *Error bars*, S.D. *D*, dephosphorylation of PrkD and PrkG by PrpC; autoradiogram showing time-dependent dephosphorylation of PrkD (*top*) and PrkG (*bottom*) by PrpC. *In vitro* kinase assays (for 20 min) were performed with PrkD and PrkG, and subsequently PrpC (~35 pmol) was added to the reactions, followed by additional incubation for different times up to 30 min at 37 °C. The corresponding SDS-PAGE images are shown in supplemental Fig. S8, *A* and *B*.

shows that the mechanism of autophosphorylation and the substrate phosphorylation in PrkG is distinct from that of PrkD and involves Thr residues in addition to Tyr residues. Therefore, PrkG is the first identified dual specificity kinase of the *Bacillus* species that can phosphorylate itself and its substrate on Ser, Thr, and Tyr residues.

Inhibition of PrkD and PrkG by Specific Inhibitors and the Effect on Cell Growth—Understanding the regulation of PrkD and PrkG by specific inhibitors can help in the development of novel drugs, which can affect the growth of *B. anthracis* by interfering with physiological function. We used several kinase inhibitors for these assays on the basis of their potency against specific eukaryotic STPK classes. Staurosporine, which acts against PKC (55), KN93 against Ca^{+2}/CaM kinase II (56), PKR inhibitor against RNA-dependent protein kinases (57), and genistein (5,7-dihydroxy-3-(4-hydroxyphenyl) chromen-4-one) against Tyr protein kinases (58) were used for these assays. Staurosporine only inhibited PrkD, and KN93 showed slight inhibition of PrkG (data not shown). Both kinases were active in the presence of the PKR inhibitor (data not shown). Under the given conditions, only genistein inhibited the kinase activity of both kinases (Fig. 7, *A* and *B*, and supplemental Fig. S7, *A* and *B*). Genistein is known to inhibit only Tyr kinases (58), which supports our previous results showing that PrkD and PrkG are regulated by Tyr phosphorylation.

To analyze the functional relevance of PrkD and PrkG inhibition by genistein and its effect on *B. anthracis*, we performed growth curve assays in the presence of genistein. The growth of *B. anthracis* cultures was inhibited by genistein at 20 and 100 μM concentrations (Fig. 7*C*). Because McsB is probably the only known Tyr kinase reported in *B. anthracis*, the observed effect could be due to concerted inhibition of McsB together with PrkD and PrkG. We subsequently used the *B. anthracis* strain, which lacks McsB (BasΔ*mcsB*) and found similar inhibitory effects by genistein on the growth of this mutant strain (supplemental Fig. S7*C*).

Role of PrpC (BA-Stp1) in Dephosphorylation of PrkD and PrkG—All cells maintain a check on protein kinases by expressing regulators, such as protein phosphatases. PrpC and its homologs have been shown to dephosphorylate and consequently regulate the activity of their cognate kinase PrkC (BA-Stk1) in both *B. subtilis* and *B. anthracis* (29, 59). Because autophosphorylation is necessary for kinase activity, PrpC-dependent dephosphorylation of the kinase can hinder downstream signaling. To determine whether PrkD and PrkG can also be inactivated by PrpC, autophosphorylated kinases were

incubated with PrpC in a time-dependent manner. PrkC, a known substrate of PrpC, was used as positive control (data not shown). Over the experimental time period, PrkG was completely dephosphorylated by PrpC, whereas the dephosphorylation of PrkD remained incomplete (Fig. 7*D* and supplemental Fig. S8, *A* and *B*). The dephosphorylation of Tyr-phosphorylated kinases indicates that PrpC, which is a Ser/Thr phosphatase, may also possess Tyr phosphatase activity. To explore this hypothesis, peptides phosphorylated at Ser, Thr, and Tyr residues were incubated individually with both His_6-tagged and GST-tagged PrpC. To our surprise, both His-tagged PrpC and GST-tagged PrpC dephosphorylated Tyr(P) peptides in addition to Ser(P) and Thr(P) peptides (supplemental Fig. S8*C*). A comparison between these phosphopeptides indicated that PrpC displays a preference for Ser(P) residues but is also able to dephosphorylate Thr(P) and Tyr(P) residues.

Identification of Pyruvate Kinase as the PrkD Substrate—To prove the DYRK-like activity of PrkD, it was necessary to show that PrkD phosphorylates its substrates on Ser/Thr and not on Tyr residue(s). To identify the substrates, we searched the homologs of *B. subtilis* phosphoproteins in *B. anthracis* (supplemental Table S3) and chose Bas4492 (BasPyk) among the predicted phosphoproteins. BasPyk is involved in the last and critical step of glycolysis, which could affect glucose metabolism. Additionally, the homolog of BasPyk in *M. tuberculosis, Mtb*PykA, was previously shown to be phosphorylated by PknJ (60). Therefore, we incubated recombinant BasPyk with PrkD in an *in vitro* kinase assay and found that it was phosphorylated (Fig. 8*A*). Importantly, no phosphorylation was observed on BasPyk by $PrkD^{K53M}$. The specificity of this observation was further shown by the lack of phosphorylation of BasPyk by PrkC and PrkG in an *in vitro* kinase assay (Fig. 8*B*). The Ser(P) and Thr(P) sites of PrkD were identified on BasPyk by PAA analysis (Fig. 8*C*). Mass spectrometry analysis revealed that BasPyk phosphorylation occurs on one Thr (Thr^9) and two Ser residues (Ser^{105} and Ser^{401}) (Fig. 8*D*). We also identified multiple additional substrates (Spo0M (Bas2153) and Bas2056) of PrkD *in vitro* and verified that phosphorylation did not occur on Tyr residues by immunoblotting with anti-Tyr(P) antibodies (data not shown).

The importance of PrkD residues, including Tyr^{182}, in the substrate phosphorylation mechanism was also verified on BasPyk. Loss of Ser^{162} and Tyr^{182} in PrkD resulted in a significant loss in BasPyk phosphorylation, which reaffirmed the role of Tyr^{182} in the kinase function (Fig. 8, *E* and *F*, and supplemental Fig. S9, *A* and *B*).

We could not identify any substrate phosphorylated by PrkG among multiple probable substrates (Ef-Tu, Ef-G, SsbA, Bas4487, and Bas1176) using the same strategy. PknG of *Corynebacterium glutamicum* is known to regulate glutamine metabolism by phosphorylating OdhI (61). Initial quantitative expression profiling data indicated that PrkG expression decreases in the presence of high concentrations of glutamine in the medium. However, experiments attempting to validate the OdhI homolog (Bas1177) as an *in vitro* substrate of PrkG failed. Therefore, additional focused genetic studies on PrkG will dissect its role in *B. anthracis* physiology.

PrkD-dependent Phosphorylation of BasPyk in Surrogate Host E. coli and Effect of Phosphorylation on Its Activity—PrkD-dependent phosphorylation on BasPyk was verified in surrogate host *E. coli* by co-expressing PrkD and BasPyk. The BasPyk was expressed in the presence of either PrkD or $PrkD^{K53M}$. Phosphorylation status of purified forms was further verified by ProQ Diamond staining, and protein amounts were validated by SYPRO® Ruby protein gel stain. PrkD phosphorylated BasPyk (Pyk-P), whereas its inactive mutant, $PrkD^{K53M}$, was unable to phosphorylate BasPyk (Pyk-UP) when expressed in *E. coli* (Fig. 9*A*). The activities of Pyk-P and Pyk-UP were further compared. Both of the proteins showed similar K_m values, but Pyk-UP exhibited higher specific activity (~25%) as compared with Pyk-P (Table 2, Fig. 9*B*, and supplemental Fig. S9*C*).

DISCUSSION

In this report, we have identified two dual specificity kinases, PrkD and PrkG, which are encoded in the genome of *B. anthracis*. Independent of its "select agent" status (62), *B. anthracis* has been projected as an outstanding model organism for studies of microbial ecology, evolution, cell development, and host-pathogen interactions (63–65). Based on the findings of this study, this medically important system can be used as a model to study signal transduction. The advantage of *B. anthracis* as a model organism is the presence of dual specificity kinases and a phosphatase together with the availability of expression analysis systems.

Quantitative real-time PCR analyses of PrkD and PrkG revealed the temporal expression profile of these kinases in various growth phases compared with PrkC. Both PrkD and PrkG are expressed in all phases of growth, indicating their possible role in the overall physiology of *B. anthracis.* The PrkD and PrkG expression levels were even higher than PrkC in the stationary phase. The expression of the three kinases at different phases alludes to the possible cross-talk between these two kinases and PrkC. Although cross-talk between STPKs has not been explored in detail, two co-expressing STPKs of *M. tuberculosis*, PknA and PknB, have been shown to undergo interdependent phosphorylation (66).

Biochemical characterization revealed the optimum conditions required for activation of PrkD and PrkG. Importantly, Mn^{2+} is required for their activation, which is also thought to be a preferred cofactor for Tyr kinases and dual specificity kinases (67, 68). To understand the regulation of these kinases, the sites of autophosphorylation were identified. Tyr phosphorylation of the two kinases was first observed by PAA analysis and immunoblotting, which was later verified by mass spectrometry. In PrkD, all of the phosphorylation sites were within the kinase domain except for Tyr^{18}. The four regulatory phosphorylation sites were found in or adjacent to the activation loop, which includes Tyr^{182}. Phosphorylation of one or more residues in the activation loop permits the kinase to refold and position for substrate binding (53). Electrostatic interactions among phosphorylated residues in the loop govern these conformational changes (53). The contribution of Ser^{162}, Thr^{180}, Thr^{181}, and Tyr^{182} was evaluated to elucidate the PrkD autophosphorylation mechanism. Whereas the loss of Thr^{180} led to enhanced phosphorylation, the loss of Ser^{162}, Thr^{181} and Tyr^{182}

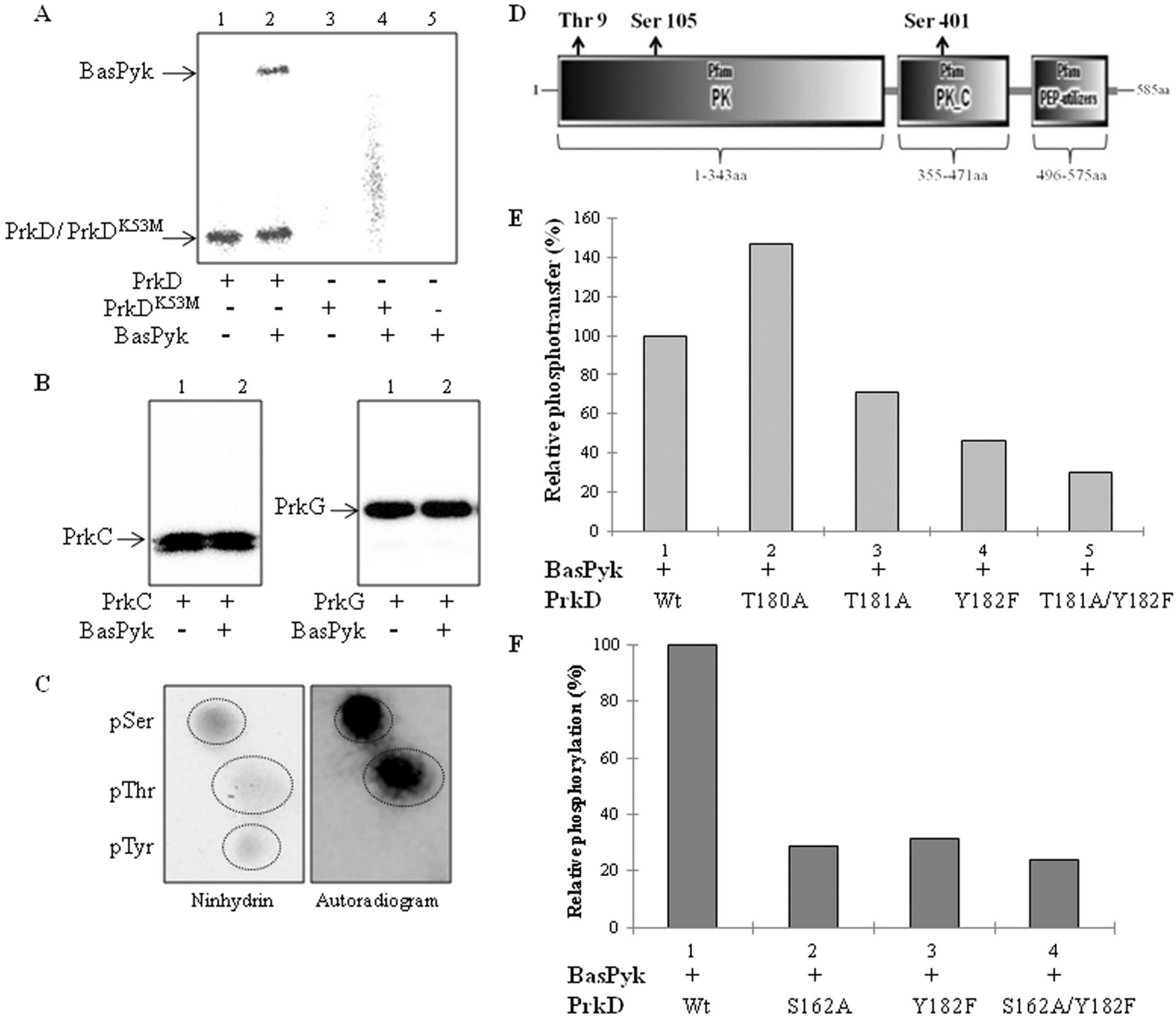

FIGURE 8. **Phosphorylation of BasPyk by PrkD.** *A*, autoradiogram showing phosphorylation of BasPyk as analyzed by *in vitro* kinase assays with PrkD. The image shows PrkD alone (*lane 1*), PrkD with BasPyk (*lane 2*), PrkD^{K53M} alone (*lane 3*), PrkD^{K53M} with BasPyk (*lane 4*), and BasPyk alone (*lane 5*). No phosphorylation was observed when PrkD^{K53M} (*lanes 3* and *4*) or BasPyk alone (*lane 5*) was used. *B*, autoradiograms showing *in vitro* kinase assays of BasPyk with PrkC (*left*) and PrkG (*right*). *Lane 1*, kinase alone; *lane 2*, kinase with BasPyk (both *panels*). *C*, PAA analysis of BasPyk phosphorylated by PrkD. *Left*, ninhydrin-stained TLC plate; *right*, corresponding autoradiogram. The ^{32}P-labeled phosphoresidues are marked in the *right panel*. *pSer*, *pThr*, and *pTyr*, phospho-Ser, -Thr, and -Tyr, respectively. *D*, domain-wise distribution of BasPyk phosphorylation sites. The PK, PK_C, and phosphoenolpyruvate utilizer domains were depicted by SMART protein domain analysis software, and phosphorylation sites are shown as Thr^{9}, Ser^{105}, and Ser^{401}. *E* and *F*, histograms showing relative phosphorylation of BasPyk by PrkD and the effect of PrkD phosphosite mutations on the phosphorylation of BasPyk. The signal intensity on BasPyk phosphorylation by wild-type PrkD was used as 100%, and relative phosphorylation was calculated by ImageGauge software. The corresponding SDS-PAGE and autoradiogram are shown in supplemental Fig. S9, *A* and *B*.

resulted in reduced autophosphorylation. Between PrkD-Thr^{181}, PrkD-Ser^{162}, and PrkD-Tyr^{182}, Tyr^{182} was found to be central to PrkD activation and overall kinase activity. Interestingly, kinase activity of another DSPK, PknD of *C. pneumoniae*, is also dependent on its activation loop residues (25). The rationale of designating Bas2152 as PrkD was its similarity to PknD, both being RD kinases.

The non-RD kinases of both pathogen and host have been implicated in pathogenesis, although RD kinases statistically outnumber them (69, 70). One such example is PknG of *M. tuberculosis*, which is also a non-RD kinase with C-terminal TPR motifs (71) and resembles the architecture of PrkG homologs from the *B. cereus* group. Based on these previous findings, we named Bas2037 as PrkG in *B. anthracis*. PknG has been shown to be phosphorylated on redox-sensing Trx (thioredoxin) motifs (71). These motifs are absent in PrkG, indicating that it must have some alternate way of activation. The only other characterized bacterial non-RD kinase is PknG of *C. glutamicum*, which is very similar to its *M. tuberculosis* homolog. In PrkG activation, multiple sites are involved, and the loss of a single site did not yield a complete loss of kinase activity. The loss of Ser^{196}, Thr^{245}, Tyr^{262}, and Tyr^{349} had a negative impact,

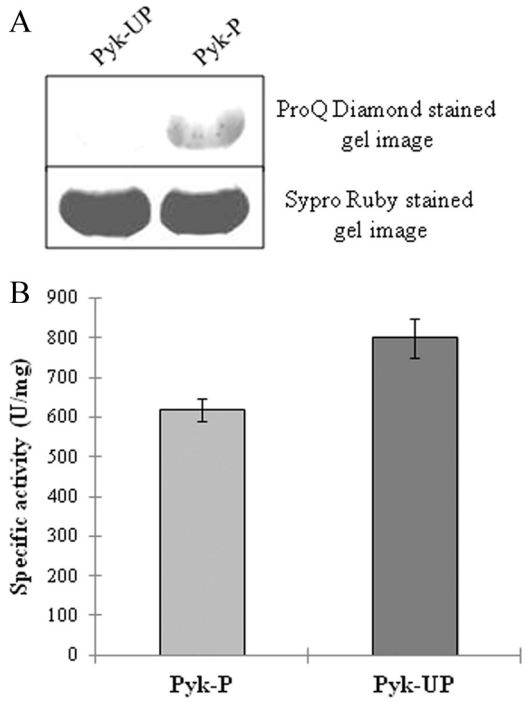

FIGURE 9. **PrkD-dependent phosphorylation of BasPyk in *E. coli* and effect of phosphorylation on BasPyk activity.** *A*, phosphospecific staining of equal amounts of phosphorylated and unphosphorylated forms of BasPyk by ProQ Diamond stain (*top*). Protein amounts were verified by Sypro Ruby staining (*bottom*). *B*, histogram comparing the specific activity of Pyk-P and Pyk-UP in units/mg of protein/min. Phosphorylated and unphosphorylated forms of BasPyk were compared in identical conditions. The experiment was performed three times, and the *error bars* represent S.D. of three individual values.

TABLE 2
K_m and specific activity of BasPyk

Enzyme	K_m ± S.D.	Specific activity ± S.D.
	mM	*units/mg protein*
Pyk-P	2.55 ± 0.21	616.9 ± 28.48
Pyk-UP	2.84 ± 0.36	800.13 ± 50.01

whereas loss of Ser^{108} had a positive effect on kinase activity of PrkG. Our results also suggest that PrkG adopts a unique activation mechanism because Tyr^{349} is located outside of the kinase domain. PrkG is the first bacterial non-RD kinase that has been shown to possess dual specificity and is a *bona fide* DSPK.

The importance of phosphorylated residues for PrkD and PrkG kinase activity was confirmed by their effect on the phosphorylation of MyBP and BasPyk substrates. PrkD phosphorylated both proteins only on Ser and Thr residues, whereas PrkG phosphorylated MyBP on Ser, Thr, and Tyr residues as identified by the PAA analysis. Phosphorylation of BasPyk was further verified by mass spectrometry of the substrate. In PrkD, three residues were found to be important for substrate phosphorylation. The first, Thr^{181}, was found to be important but not necessary for autophosphorylation but was found to be necessary for substrate phosphorylation. The other two, more critical, residues in PrkD activation were Ser^{162} and Tyr^{182}, the loss of which is insurmountable for autophosphorylation and substrate phosphorylation.

As previously discussed, PrkD homologs exist in all *Bacillus* species, but Tyr^{182} is absent in all species except for the *B. cereus* group. The Tyr phosphorylation activity of PrkD was restricted to autophosphorylation. On the basis of these results, we report PrkD as a protein kinase similar to the DYRK class of kinases, which is an undiscovered enzyme class of the bacterial world. In eukaryotes, the DYRK class of kinases is known to regulate critical cellular functions, such as controlling the cell cycle, cytokinesis, cell differentiation, and brain development (34, 35, 72–74). Eukaryotic DYRKs are known to target the RP*X*(S/T)P motif with a preference for Pro at the P+1 position and Arg at the P−3 position (75). In PrkD, Arg^{15}, Arg^{178}, and Pro^{246} may assist in the phosphorylation of Thr^{18}, Thr^{181}, and Thr^{245}, respectively. Importantly, these residues are also conserved in *B. cereus* group homologs and absent in the *B. subtilis* homolog (supplemental Fig. S10). Additionally, the absence of characteristic DYRK motifs, such as the DYRK homology box, N-terminal autophosphorylation accessory region, and motif rich in Pro, Glu, Ser, and Thr residues (PEST) in PrkD, indicates that although they behave similarly, their regulatory mechanism may not be identical. Although we have observed profound similarities between PrkD and the DYRK class of kinases, further structural evidence is required to identify all variations of this enzyme. PrkG activation seems to be quite complex and is dependent on multiple residues. The two critical residues Tyr^{349} and Thr^{245} are located so distant from each other that further structural evidence is required to fully understand the activation and substrate binding mechanisms.

The present study also provides evidence of the dual specific nature of PrpC, which is the only Ser/Thr protein phosphatase in *B. anthracis*. In bacteria, Ser/Thr phosphatases are known to inactivate their cognate kinases, and thus their role is directly proportional to the importance of the kinase with which they are involved. PrpC was previously shown to be important for *B. anthracis* and *B. subtilis* as a partner of PrkC (29, 59). Our results demonstrate that PrpC can also dephosphorylate the dual specificity protein kinases and may have a broader role beyond PrkC in *B. anthracis*. Interestingly, the Ser/Thr phosphatase PrpZ from *Salmonella enterica* also showed a similar dual specific nature with Tyr(P) peptides, but its protein substrates remain unknown (76).

The inhibition of PrkD and PrkG by genistein was used to study the physiological significance of these enzymes. *B. anthracis* vegetative cell growth was inhibited in the presence of 20 μM genistein, which became more significant at 100 μM. Similar effects on *B. anthracis* growth were also reported for genistein by Hong *et al.* (77). Furthermore, identification of BasPyk as a substrate of PrkD provides initial insight of the role of this kinase in glucose metabolism.

Identification of BasPyk as a substrate of PrkD in the *in vitro* conditions as well as in the surrogate host *E. coli* provides initial insights into the role of this kinase. The phosphorylated form of BasPyk was purified by co-expressing with the kinase. Compared with its unphosphorylated form, the phosphorylated BasPyk showed a reduced rate of product formation (V_{max}) and specific activity. The decrease in BasPyk specific activity may influence the phosphoenolpyruvate catabolism. In addition, pyruvate being an important metabolite, any variation in its concentration may affect several metabolic pathways.

In conclusion, we found that PrkD is conserved throughout the *Bacillus* species, but only the homologs present in the *B. cereus* group have a conserved Tyr residue in the activation loop. PrkG is present only in the *B. cereus* group and is expressed with a kinase domain lacking the TPR region at the C terminus in most of the *B. anthracis* strains sequenced so far. We hypothesize that specialization of *B. anthracis* as a warm blooded animal pathogen may have reduced the range of environmental stimuli to which it was exposed. This may have led to the loss of some Tyr kinases, which ultimately resulted in the evolution of dual specificity enzymes.

Acknowledgments—We thank Prof. Charles L. Turnbough, Jr. (University of Alabama at Birmingham) for support. We also thank Landon Wilson and the University of Alabama at Birmingham Mass Spectrometry Core Facility for performing LC-MS/MS analyses for the identification of phosphorylation sites. We also thank Dr. Christopher Brooks (Bioscience Editing Solutions services) for help and for editing the manuscript.

REFERENCES

1. Cozzone, A. J. (2005) Role of protein phosphorylation on serine/threonine and tyrosine in the virulence of bacterial pathogens. *J. Mol. Microbiol. Biotechnol.* **9,** 198–213
2. Parkinson, J. S. (1993) Signal transduction schemes of bacteria. *Cell* **73,** 857–871
3. Pereira, S. F., Goss, L., and Dworkin, J. (2011) Eukaryote-like serine/threonine kinases and phosphatases in bacteria. *Microbiol. Mol. Biol. Rev.* **75,** 192–212
4. Chakraborti, P. K., Matange, N., Nandicoori, V. K., Singh, Y., Tyagi, J. S., and Visweswariah, S. S. (2011) Signaling mechanisms in Mycobacteria. *Tuberculosis* **91,** 432–440
5. Alber, T. (2009) Signaling mechanisms of the *Mycobacterium tuberculosis* receptor Ser/Thr protein kinases. *Curr. Opin. Struct. Biol.* **19,** 650–657
6. Danilenko, V. N., Osolodkin, D. I., Lakatosh, S. A., Preobrazhenskaya, M. N., and Shtil, A. A. (2011) Bacterial eukaryotic type serine-threonine protein kinases. From structural biology to targeted anti-infective drug design. *Curr. Top. Med. Chem.* **11,** 1352–1369
7. Molle, V., and Kremer, L. (2010) Division and cell envelope regulation by Ser/Thr phosphorylation. Mycobacterium shows the way. *Mol. Microbiol.* **75,** 1064–1077
8. Wehenkel, A., Bellinzoni, M., Graña, M., Duran, R., Villarino, A., Fernandez, P., Andre-Leroux, G., England, P., Takiff, H., Cerveñansky, C., Cole, S. T., and Alzari, P. M. (2008) Mycobacterial Ser/Thr protein kinases and phosphatases. Physiological roles and therapeutic potential. *Biochim. Biophys. Acta* **1784,** 193–202
9. Hanks, S. K., and Hunter, T. (1995) Protein kinases 6. The eukaryotic protein kinase superfamily. Kinase (catalytic) domain structure and classification. *FASEB J.* **9,** 576–596
10. Av-Gay, Y., and Everett, M. (2000) The eukaryotic-like Ser/Thr protein kinases of *Mycobacterium tuberculosis*. *Trends Microbiol.* **8,** 238–244
11. Bechet, E., Guiral, S., Torres, S., Mijakovic, I., Cozzone, A. J., and Grangeasse, C. (2009) Tyrosine-kinases in bacteria. From a matter of controversy to the status of key regulatory enzymes. *Amino Acids* **37,** 499–507
12. Grangeasse, C., Cozzone, A. J., Deutscher, J., and Mijakovic, I. (2007) Tyrosine phosphorylation. An emerging regulatory device of bacterial physiology. *Trends Biochem. Sci.* **32,** 86–94
13. Kiley, T. B., and Stanley-Wall, N. R. (2010) Post-translational control of *Bacillus subtilis* biofilm formation mediated by tyrosine phosphorylation. *Mol. Microbiol.* **78,** 947–963
14. Kirstein, J., and Turgay, K. (2005) A new tyrosine phosphorylation mechanism involved in signal transduction in *Bacillus subtilis*. *J. Mol. Microbiol. Biotechnol.* **9,** 182–188
15. Lacour, S., Bechet, E., Cozzone, A. J., Mijakovic, I., and Grangeasse, C. (2008) Tyrosine phosphorylation of the UDP-glucose dehydrogenase of *Escherichia coli* is at the crossroads of colanic acid synthesis and polymyxin resistance. *PLoS One* **3,** e3053
16. Lee, D. C., and Jia, Z. (2009) Emerging structural insights into bacterial tyrosine kinases. *Trends Biochem. Sci.* **34,** 351–357
17. Mijakovic, I., Petranovic, D., Bottini, N., Deutscher, J., and Ruhdal Jensen, P. (2005) Protein-tyrosine phosphorylation in *Bacillus subtilis*. *J. Mol. Microbiol. Biotechnol.* **9,** 189–197
18. Petranovic, D., Michelsen, O., Zahradka, K., Silva, C., Petranovic, M., Jensen, P. R., and Mijakovic, I. (2007) *Bacillus subtilis* strain deficient for the protein-tyrosine kinase PtkA exhibits impaired DNA replication. *Mol. Microbiol.* **63,** 1797–1805
19. Grangeasse, C., Terreux, R., and Nessler, S. (2010) Bacterial tyrosine-kinases. Structure-function analysis and therapeutic potential. *Biochim. Biophys. Acta* **1804,** 628–634
20. Jadeau, F., Bechet, E., Cozzone, A. J., Deléage, G., Grangeasse, C., and Combet, C. (2008) Identification of the idiosyncratic bacterial protein tyrosine kinase (BY-kinase) family signature. *Bioinformatics* **24,** 2427–2430
21. Lee, D. C., Zheng, J., She, Y. M., and Jia, Z. (2008) Structure of *Escherichia coli* tyrosine kinase Etk reveals a novel activation mechanism. *EMBO J.* **27,** 1758–1766
22. Olivares-Illana, V., Meyer, P., Bechet, E., Gueguen-Chaignon, V., Soulat, D., Lazereg-Riquier, S., Mijakovic, I., Deutscher, J., Cozzone, A. J., Laprévote, O., Morera, S., Grangeasse, C., and Nessler, S. (2008) Structural basis for the regulation mechanism of the tyrosine kinase CapB from *Staphylococcus aureus*. *PLoS Biol.* **6,** e143
23. Fuhrmann, J., Schmidt, A., Spiess, S., Lehner, A., Turgay, K., Mechtler, K., Charpentier, E., and Clausen, T. (2009) McsB is a protein arginine kinase that phosphorylates and inhibits the heat-shock regulator CtsR. *Science* **324,** 1323–1327
24. Kirstein, J., Zühlke, D., Gerth, U., Turgay, K., and Hecker, M. (2005) A tyrosine kinase and its activator control the activity of the CtsR heat shock repressor in *B. subtilis*. *EMBO J.* **24,** 3435–3445
25. Johnson, D. L., and Mahony, J. B. (2007) *Chlamydophila pneumoniae* PknD exhibits dual amino acid specificity and phosphorylates Cpn0712, a putative type III secretion YscD homolog. *J. Bacteriol.* **189,** 7549–7555
26. Low, H., Chua, C. S., and Sim, T. S. (2012) *Plasmodium falciparum* possesses a unique dual specificity serine/threonine and tyrosine kinase, Pfnek3. *Cell Mol. Life Sci.* **69,** 1523–1535
27. Ostrovsky, P. C., and Maloy, S. (1995) Protein phosphorylation on serine, threonine, and tyrosine residues modulates membrane-protein interactions and transcriptional regulation in *Salmonella typhimurium*. *Genes Dev.* **9,** 2034–2041
28. Madec, E., Laszkiewicz, A., Iwanicki, A., Obuchowski, M., and Séror, S. (2002) Characterization of a membrane-linked Ser/Thr protein kinase in *Bacillus subtilis*, implicated in developmental processes. *Mol. Microbiol.* **46,** 571–586
29. Shakir, S. M., Bryant, K. M., Larabee, J. L., Hamm, E. E., Lovchik, J., Lyons, C. R., and Ballard, J. D. (2010) Regulatory interactions of a virulence-associated serine/threonine phosphatase-kinase pair in *Bacillus anthracis*. *J. Bacteriol.* **192,** 400–409
30. Bryant-Hudson, K. M., Shakir, S. M., and Ballard, J. D. (2011) Autoregulatory characteristics of a *Bacillus anthracis* serine/threonine kinase. *J. Bacteriol.* **193,** 1833–1842
31. Shah, I. M., Laaberki, M. H., Popham, D. L., and Dworkin, J. (2008) A eukaryotic-like Ser/Thr kinase signals bacteria to exit dormancy in response to peptidoglycan fragments. *Cell* **135,** 486–496
32. Mattoo, A. R., Arora, A., Maiti, S., and Singh, Y. (2008) Identification, characterization, and activation mechanism of a tyrosine kinase of *Bacillus anthracis*. *FEBS J.* **275,** 6237–6247
33. de Been, M., Francke, C., Moezelaar, R., Abee, T., and Siezen, R. J. (2006) Comparative analysis of two-component signal transduction systems of *Bacillus cereus*, *Bacillus thuringiensis*, and *Bacillus anthracis*. *Microbiology* **152,** 3035–3048
34. Aranda, S., Laguna, A., and de la Luna, S. (2011) DYRK family of protein kinases. Evolutionary relationships, biochemical properties, and functional roles. *FASEB J.* **25,** 449–462

35. Becker, W., and Joost, H. G. (1999) Structural and functional characteristics of Dyrk, a novel subfamily of protein kinases with dual specificity. *Prog. Nucleic Acid Res. Mol. Biol.* **62,** 1–17
36. Dhanasekaran, N., and Premkumar Reddy, E. (1998) Signaling by dual specificity kinases. *Oncogene* **17,** 1447–1455
37. Douville, E., Duncan, P., Abraham, N., and Bell, J. C. (1994) Dual specificity kinases. A new family of signal transducers. *Cancer Metastasis Rev.* **13,** 1–7
38. Jahn, C. E., Charkowski, A. O., and Willis, D. K. (2008) Evaluation of isolation methods and RNA integrity for bacterial RNA quantitation. *J. Microbiol. Methods* **75,** 318–324
39. Schmitt, M. E., Brown, T. A., and Trumpower, B. L. (1990) A rapid and simple method for preparation of RNA from *Saccharomyces cerevisiae*. *Nucleic Acids Res.* **18,** 3091–3092
40. Yang, F., Tan, H., Zhou, Y., Lin, X., and Zhang, S. (2011) High quality RNA preparation from *Rhodosporidium toruloides* and cDNA library construction therewith. *Mol. Biotechnol.* **47,** 144–151
41. Passalacqua, K. D., Bergman, N. H., Herring-Palmer, A., and Hanna, P. (2006) The superoxide dismutases of *Bacillus anthracis* do not cooperatively protect against endogenous superoxide stress. *J. Bacteriol.* **188,** 3837–3848
42. Gupta, M., Sajid, A., Arora, G., Tandon, V., and Singh, Y. (2009) Forkhead-associated domain-containing protein Rv0019c and polyketide-associated protein PapA5, from substrates of serine/threonine protein kinase PknB to interacting proteins of *Mycobacterium tuberculosis*. *J. Biol. Chem.* **284,** 34723–34734
43. Koul, A., Choidas, A., Tyagi, A. K., Drlica, K., Singh, Y., and Ullrich, A. (2001) Serine/threonine protein kinases PknF and PknG of *Mycobacterium tuberculosis*. Characterization and localization. *Microbiology* **147,** 2307–2314
44. Sajid, A., Arora, G., Gupta, M., Upadhyay, S., Nandicoori, V. K., and Singh, Y. (2011) Phosphorylation of *Mycobacterium tuberculosis* Ser/Thr phosphatase by PknA and PknB. *PLoS One* **6,** e17871
45. Pomerantsev, A. P., Pomerantseva, O. M., Moayeri, M., Fattah, R., Tallant, C., and Leppla, S. H. (2011) A *Bacillus anthracis* strain deleted for six proteases serves as an effective host for production of recombinant proteins. *Protein Expr. Purif.* **80,** 80–90
46. Boyle, W. J., van der Geer, P., and Hunter, T. (1991) Phosphopeptide mapping and phosphoamino acid analysis by two-dimensional separation on thin layer cellulose plates. *Methods Enzymol.* **201,** 110–149
47. McPherson, S. A., Li, M., Kearney, J. F., and Turnbough, C. L., Jr. (2010) ExsB, an unusually highly phosphorylated protein required for the stable attachment of the exosporium of *Bacillus anthracis*. *Mol. Microbiol.* **76,** 1527–1538
48. Khan, S., Nagarajan, S. N., Parikh, A., Samantaray, S., Singh, A., Kumar, D., Roy, R. P., Bhatt, A., and Nandicoori, V. K. (2010) Phosphorylation of enoyl-acyl carrier protein reductase InhA impacts mycobacterial growth and survival. *J. Biol. Chem.* **285,** 37860–37871
49. Sajid, A., Arora, G., Gupta, M., Singhal, A., Chakraborty, K., Nandicoori, V. K., and Singh, Y. (2011) Interaction of *Mycobacterium tuberculosis* elongation factor Tu with GTP is regulated by phosphorylation. *J. Bacteriol.* **193,** 5347–5358
50. Johnsen, U., Hansen, T., and Schonheit, P. (2003) Comparative analysis of pyruvate kinases from the hyperthermophilic archaea *Archaeoglobus fulgidus*, *Aeropyrum pernix*, and *Pyrobaculum aerophilum* and the hyperthermophilic bacterium *Thermotoga maritima*. Unusual regulatory properties in hyperthermophilic archaea. *J. Biol. Chem.* **278,** 25417–25427
51. Malcovati, M., and Valentini, G. (1982) AMP- and fructose 1,6-bisphosphate-activated pyruvate kinases from *Escherichia coli*. *Methods Enzymol.* **90,** 170–179
52. Johnson, L. N., Noble, M. E., and Owen, D. J. (1996) Active and inactive protein kinases. Structural basis for regulation. *Cell* **85,** 149–158
53. Nolen, B., Taylor, S., and Ghosh, G. (2004) Regulation of protein kinases. Controlling activity through activation segment conformation. *Mol. Cell* **15,** 661–675
54. Liu, H., Bergman, N. H., Thomason, B., Shallom, S., Hazen, A., Crossno, J., Rasko, D. A., Ravel, J., Read, T. D., Peterson, S. N., Yates, J., 3rd, and Hanna, P. C. (2004) Formation and composition of the *Bacillus anthracis* endospore. *J. Bacteriol.* **186,** 164–178
55. Tamaoki, T., Nomoto, H., Takahashi, I., Kato, Y., Morimoto, M., and Tomita, F. (1986) Staurosporine, a potent inhibitor of phospholipid/Ca^{2+}-dependent protein kinase. *Biochem. Biophys. Res. Commun.* **135,** 397–402
56. Rokolya, A., and Singer, H. A. (2000) Inhibition of CaM kinase II activation and force maintenance by KN-93 in arterial smooth muscle. *Am. J. Physiol. Cell Physiol.* **278,** C537–C545
57. Ruvolo, V. R., Kurinna, S. M., Karanjeet, K. B., Schuster, T. F., Martelli, A. M., McCubrey, J. A., and Ruvolo, P. P. (2008) PKR regulates B56α-mediated BCL2 phosphatase activity in acute lymphoblastic leukemia-derived REH cells. *J. Biol. Chem.* **283,** 35474–35485
58. Akiyama, T., Ishida, J., Nakagawa, S., Ogawara, H., Watanabe, S., Itoh, N., Shibuya, M., and Fukami, Y. (1987) Genistein, a specific inhibitor of tyrosine-specific protein kinases. *J. Biol. Chem.* **262,** 5592–5595
59. Gaidenko, T. A., Kim, T. J., and Price, C. W. (2002) The PrpC serine-threonine phosphatase and PrkC kinase have opposing physiological roles in stationary phase *Bacillus subtilis* cells. *J. Bacteriol.* **184,** 6109–6114
60. Arora, G., Sajid, A., Gupta, M., Bhaduri, A., Kumar, P., Basu-Modak, S., and Singh, Y. (2010) Understanding the role of PknJ in *Mycobacterium tuberculosis*. Biochemical characterization and identification of novel substrate pyruvate kinase A. *PLoS One* **5,** e10772
61. Niebisch, A., Kabus, A., Schultz, C., Weil, B., and Bott, M. (2006) Corynebacterial protein kinase G controls 2-oxoglutarate dehydrogenase activity via the phosphorylation status of the OdhI protein. *J. Biol. Chem.* **281,** 12300–12307
62. Dias, M. B., Reyes-Gonzalez, L., Veloso, F. M., and Casman, E. A. (2010) Effects of the USA PATRIOT Act and the 2002 Bioterrorism Preparedness Act on select agent research in the United States. *Proc. Natl. Acad. Sci. U.S.A.* **107,** 9556–9561
63. Koehler, T. M. (2009) *Bacillus anthracis* physiology and genetics. *Mol. Aspects Med.* **30,** 386–396
64. Barth, H., Aktories, K., Popoff, M. R., and Stiles, B. G. (2004) Binary bacterial toxins. Biochemistry, biology, and applications of common *Clostridium* and *Bacillus* proteins. *Microbiol. Mol. Biol. Rev.* **68,** 373–402, table of contents
65. Keim, P. S., and Wagner, D. M. (2009) Humans and evolutionary and ecological forces shaped the phylogeography of recently emerged diseases. *Nat. Rev. Microbiol.* **7,** 813–821
66. Kang, C. M., Abbott, D. W., Park, S. T., Dascher, C. C., Cantley, L. C., and Husson, R. N. (2005) The *Mycobacterium tuberculosis* serine/threonine kinases PknA and PknB. Substrate identification and regulation of cell shape. *Genes Dev.* **19,** 1692–1704
67. Chardot, T., Shen, H., and Meunier, J. C. (1995) Dual specificity of casein kinase II from the yeast *Yarrowia lipolytica*. *C. R. Acad. Sci. III* **318,** 937–942
68. Reddy, M. M., and Rajasekharan, R. (2006) Role of threonine residues in the regulation of manganese-dependent *Arabidopsis* serine/threonine/tyrosine protein kinase activity. *Arch. Biochem. Biophys.* **455,** 99–109
69. Dardick, C., and Ronald, P. (2006) Plant and animal pathogen recognition receptors signal through non-RD kinases. *PLoS Pathog.* **2,** e2
70. Walburger, A., Koul, A., Ferrari, G., Nguyen, L., Prescianotto-Baschong, C., Huygen, K., Klebl, B., Thompson, C., Bacher, G., and Pieters, J. (2004) Protein kinase G from pathogenic mycobacteria promotes survival within macrophages. *Science* **304,** 1800–1804
71. Tiwari, D., Singh, R. K., Goswami, K., Verma, S. K., Prakash, B., and Nandicoori, V. K. (2009) Key residues in *Mycobacterium tuberculosis* protein kinase G play a role in regulating kinase activity and survival in the host. *J. Biol. Chem.* **284,** 27467–27479
72. Canzonetta, C., Mulligan, C., Deutsch, S., Ruf, S., O'Doherty, A., Lyle, R., Borel, C., Lin-Marq, N., Delom, F., Groet, J., Schnappauf, F., De Vita, S., Averill, S., Priestley, J. V., Martin, J. E., Shipley, J., Denyer, G., Epstein, C. J., Fillat, C., Estivill, X., Tybulewicz, V. L., Fisher, E. M., Antonarakis, S. E., and Nizetic, D. (2008) DYRK1A dosage imbalance perturbs NRSF/REST levels, deregulating pluripotency and embryonic stem cell fate in Down syndrome. *Am. J. Hum. Genet.* **83,** 388–400
73. Hachet, O., Berthelot-Grosjean, M., Kokkoris, K., Vincenzetti, V., Moosbrugger, J., and Martin, S. G. (2011) A phosphorylation cycle shapes gradients of the DYRK family kinase Pom1 at the plasma membrane. *Cell* **145,** 1116–1128

74. Yang, E. J., Ahn, Y. S., and Chung, K. C. (2001) Protein kinase Dyrk1 activates cAMP response element-binding protein during neuronal differentiation in hippocampal progenitor cells. *J. Biol. Chem.* **276,** 39819–39824
75. Himpel, S., Tegge, W., Frank, R., Leder, S., Joost, H. G., and Becker, W. (2000) Specificity determinants of substrate recognition by the protein kinase DYRK1A. *J. Biol. Chem.* **275,** 2431–2438
76. Lai, S. M., and Le Moual, H. (2005) PrpZ, a *Salmonella enterica* serovar Typhi serine/threonine protein phosphatase 2C with dual substrate specificity. *Microbiology* **151,** 1159–1167
77. Hong, H., Landauer, M. R., Foriska, M. A., and Ledney, G. D. (2006) Antibacterial activity of the soy isoflavone genistein. *J. Basic Microbiol.* **46,** 329–335